Renormalization-group flow equations of model F

Volker Dohm
Institut für Theoretische Physik, Technische Hochschule Aachen, D-5100 Aachen, Germany
(Received 21 November 1990)

The dynamic renormalization-group flow equations for model F of Halperin, Hohenberg, and Siggia [Phys. Rev. B **13**, 1299 (1976)] are calculated by means of renormalized field theory within the minimal-renormalization scheme up to two-loop order. These equations are combined with the Borel-resummation results for the static renormalization-group functions computed by Schloms and Dohm. The corresponding static fixed point destabilizes the dynamic-scaling fixed point in two-loop order. The nonuniversal initial values of the static and dynamic flow equations are identified for the λ transition of ^{4}He at various pressures. Predictions are made for the bulk thermal conductivity very close to T_λ where the departures from dynamic scaling should be observable. Effective static and dynamic parameters are computed that can be applied to other critical phenomena above and below the λ line of ^{4}He.

I. INTRODUCTION

It is well known that the ideal properties of the superfluid transition of ^{4}He provide a unique opportunity to test the renormalization-group (RG) theory of dynamic critical phenomena[1–3] in a highly quantitative sense. In recent years the experimental accuracy has reached a level which permits us to measure not only dynamic bulk phenomena with improved resolution but also dynamic finite-size, nonequilibrium, and nonlinear properties deeply in the critical region (for a review see Ref. 4). These high-resolution measurements reveal new physical effects and open up the possibility of testing new aspects of the RG theory which have previously not been amenable to experimental verification.

The theoretical description of these phenomena is based on the RG transformation which maps correlation (and response) functions from the critical to the noncritical region. This transformation implies a decomposition of a correlation function into an exponential integral times an amplitude function that depends on effective dimensionless couplings $c_i(l)$. The details of this decomposition depend on the particular renormalization procedure employed. We shall use the field-theoretic RG approach[5] within the minimal subtraction scheme[6–9] which provides important simplifications in calculations beyond lowest order. The effective couplings $c_i(l)$ satisfy RG flow equations

$$l\frac{dc_i(l)}{dl}=\beta_{c_i}(\{c(l)\}) , \tag{1.1}$$

where the dimensionless flow parameter l varies between $l\simeq O(1)$ (noncritical background) and $l=0$ (asymptotic criticality).

It is expected that sufficiently close to the superfluid transition of ^{4}He a complete description of the low-frequency critical dynamics is provided by the so-called model F[10,11] of Halperin, Hohenberg, and Siggia and by appropriate extensions thereof. The extensions may include the effect of restricted geometries and of external heat sources,[12,13] the first-sound[14] and the shear modes,[15] the ^{3}He concentration,[16,17] and the effects of vortices (such as mutual friction).[18] The effective static[19] and dynamic[11] couplings $c_i(l)$ of model F are (i) the four-point coupling $u(l)$ of the Landau-Ginzburg-Wilson functional, (ii) the coupling $\gamma(l)$ between the order parameter ψ_0 and the entropy variable m_0, (iii) the reversible dynamic coupling $F(l)$ between ψ_0 and m_0, (iv) the effective ratio $w'(l)$ of relaxation rates of ψ_0 and m_0, and (v) an effective nondissipative dynamic coupling $w''(l)$ which originates from the equations of motion of an interacting Bose system.[20] It is customary to combine $w'(l)$ and $w''(l)$ in a complex parameter $w(l)=w'(l)+iw''(l)$. Thus for model F the couplings $c_i(l)$ in (1.1) are

$$\{c(l)\}=u(l),\gamma(l),F(l),w(l) . \tag{1.2}$$

The flow parameter l can be interpreted as a distance from criticality not only in the sense that $l=l(t)$ depends on the reduced temperature $t=(T-T_\lambda)/T_\lambda$ but more generally

$$l=l(t,k,L^{-1},\omega,Q_0) . \tag{1.3}$$

Here we consider a parameter space spanned by the experimental controllable parameters t,k (wave number), ω (frequency), L^{-1} (inverse size of the system), and by a nonequilibrium parameter Q_0 (such as an external heat current) which drives the system away from the equilibrium. Criticality ($l=0$) is reached only as each of these parameters tends to zero. It is important to realize that, within the minimal subtraction scheme, the functions $\beta_{c_i}(\{c\})$ *do not depend on the parameters* t,k,L^{-1},ω,Q_0, thus the variety of different critical phenomena in the entire (t,k,L^{-1},ω,Q_0)-parameter space above and below T_λ is governed by the *same* set of RG flow equations (1.1). Clearly the calculation of the corresponding functions β_u, β_γ, β_F, and β_w is a crucial ingredient of the theory which has considerable impact on all dynamic critical phenomena along the λ line of ^{4}He (as well as for systems within the same universality class like the XY transition of MnF_2

above the bicritical point.[21]

The static functions β_u and β_γ have been computed recently[8] by means of the Borel resummation method, and the dynamic function β_F has been calculated in Ref. 11 up to two-loop order. The most complicated part of the flow equations, however, consists of the complex function β_w. In this paper we publish the missing information on β_w as derived from a complete two-loop calculation.

So far this function β_w was available only in an unpublished report.[22] The effective parameters $w(l)$ and $F(l)$ obtained from the two-loop functions β_w and β_F and the ensuing theoretical predictions have been used and discussed already in a number of papers[2–4,12–15,20,23–33] as well as in unpublished work.[34–39] We expect that the RG flow equations of model F will remain relevant also in future developments (e.g., dynamic finite-size and surface effects, nonlinear and nonequilibrium phenomena, dynamic critical effects of vortices, analysis of very high resolution experiments on bulk transport coefficients).

A special motivation for publishing our calculation is due to recent high-resolution measurements of the bulk thermal conductivity above T_λ.[27] These data are in serious disagreement with the theoretical prediction based on our two-loop model-F calculation. This disagreement does not seem to be explainable in terms of surface or finite-size effects as indicated by recent calculations[13] and by measurements of the Kapitza resistance above T_λ.[40]

In Sec. II we introduce our notation and definitions. The two-loop result for β_w is presented in Sec. III and the instability of the dynamic-scaling fixed point is briefly discussed. In Sec. IV the procedure is described how to determine the effective parameters for the superfluid transition of ^{4}He, and predictions are made for the bulk thermal conductivity very close to T_λ at several pressures. The appendixes contain the main information on the two-loop calculation and on the numerical results for the effective static and dynamic parameters.

II. MODEL AND DEFINITIONS

We consider the following set of coupled Langevin equations for the complex order parameter $\psi_0(x,t)$ and the conserved secondary variable $m_0(x,t)$ as introduced by Halperin, Hohenberg, and Siggia:[10]

$$\frac{\partial}{\partial t}\psi_0(x,t) = -2\Gamma_0\frac{\delta H}{\delta\psi_0^*} + ig_0\psi_0\frac{\delta H}{\delta m_0} + \Theta_\psi , \tag{2.1}$$

$$\frac{\partial}{\partial t}m_0(x,t) = \lambda_0\nabla^2\frac{\delta H}{\delta m_0} - 2g_0\,\mathrm{Im}\left[\psi_0^*\frac{\delta H}{\delta\psi_0^*}\right] + \Theta_m , \tag{2.2}$$

$$H = \int d^dx\left(\tfrac{1}{2}\tau_0|\psi_0|^2 + \tfrac{1}{2}|\nabla\psi_0|^2 + \tilde{u}_0|\psi_0|^4 + \tfrac{1}{2}\chi_0^{-1}m_0^2 + \gamma_0 m_0|\psi_0|^2 - h_0 m_0\right) . \tag{2.3}$$

The Gaussian Langevin forces have the nonvanishing correlations

$$\langle\Theta_\psi(x,t)\Theta_\psi^*(0,0)\rangle = 4\Gamma_0'\delta(x)\delta(t) , \tag{2.4}$$

$$\langle\Theta_m(x,t)\Theta_m(0,0)\rangle = -2\lambda_0\nabla^2\delta(x)\delta(t) . \tag{2.5}$$

Throughout this paper we use the notation and sign convention of Refs. 11 and 19. Instead of $\tilde{u}_0$ and τ_0 we shall employ

$$u_0 = \tilde{u}_0 - \tfrac{1}{2}\gamma_0^2\chi_0 \tag{2.6}$$

and

$$r_0 = \tau_0 + 2\gamma_0 h_0\chi_0 , \tag{2.7}$$

where we consider h_0 as a function of τ_0, γ_0, and $\tilde{u}_0$ or u_0 [see (A25) in Appendix A]. We define the following renormalized quantities:

$$\psi = Z_\psi^{-1/2}\psi_0 , \tag{2.8}$$

$$r = Z_r^{-1}(r_0 - r_{0C}) , \tag{2.9}$$

$$u = \mu^{-\epsilon}Z_u^{-1}Z_\psi^2 A_d u_0, \tag{2.10}$$

$$m = Z_m^{-1/2}\chi_0^{-1/2}m_0 , \tag{2.11}$$

$$\gamma = \mu^{-\epsilon/2}Z_m^{-1/2}Z_r^{-1}A_d^{1/2}\chi_0^{1/2}\gamma_0 , \tag{2.12}$$

$$\lambda = Z_\lambda\lambda_0\chi_0^{-1} , \tag{2.13}$$

$$\Gamma = Z_\Gamma\Gamma_0 , \tag{2.14}$$

$$g = \mu^{-\epsilon/2}Z_m^{-1/2}A_d^{1/2}g_0\chi_0^{-1/2} , \tag{2.15}$$

with $\epsilon = 4-d$ and the geometrical factor[11,19]

$$A_d = \frac{\Gamma(3-d/2)}{2^{d-2}\pi^{d/2}(d-2)} . \tag{2.16}$$

The various Z factors are functions only of the dimensionless renormalized parameters u, γ, and

$$w = \Gamma/\lambda = w' + iw'' , \tag{2.17}$$

$$F = g/\lambda . \tag{2.18}$$

Explicit expressions for the Z factors in the minimal subtraction scheme are given in Appendix C. The parameter μ^{-1} is an arbitrary reference length of the renormalized theory. We need the following static and dynamic renormalization-group functions:

$$\beta_u(u) = (\mu\partial_\mu u)_0 , \tag{2.19}$$

$$\zeta_r(u) = (\mu\partial_\mu \ln Z_r^{-1})_0 , \tag{2.20}$$

$$\zeta_m(\gamma,\mu) = (\mu\partial_\mu \ln Z_m^{-1})_0 , \tag{2.21}$$

$$\zeta_\lambda(w,F,\gamma,u) = (\mu\partial_\mu \ln Z_\lambda)_0 , \tag{2.22}$$

$$\zeta_\Gamma(w,F,\gamma,\mu) = (\mu\partial_\mu \ln Z_\Gamma)_0 . \tag{2.23}$$

The differentiations in (2.19)–(2.23) are taken at fixed unrenormalized parameters. The parameters u, γ, F, and w' are real and non-negative. The complex conjugate of w will be denoted by

$$w^* = \frac{\Gamma^*}{\lambda} = w' - iw'' \tag{2.24}$$

which should not be confused with the fixed point value of w. The real and imaginary parts of the latter will be denoted by $(w')^*$ and $(w'')^*$, see (3.35) and (3.41).

III. RENORMALIZATION-GROUP FLOW EQUATIONS

A. General form

The effective dynamic parameters $w(l)$ and $F(l)$ are defined as the solutions of the following renormalization-group flow equations:

$$l\frac{dw(l)}{dl}=\beta_w(w(l),F(l),\gamma(l),u(l)) , \tag{3.1}$$

$$l\frac{dF(l)}{dl}=\beta_F(w(l),F(l),\gamma(l),u(l)) . \tag{3.2}$$

The effective static parameters $u(l)$ and $\gamma(l)$ in (3.1) and (3.2) are independent of $w(l)$ and $F(l)$ and are the solutions of

$$l\frac{du(l)}{dl}=\beta_u(u(l)) , \tag{3.3}$$

$$l\frac{d\gamma(l)}{dl}=\beta_\gamma(\gamma(l),u(l)) . \tag{3.4}$$

The flow parameter l may vary between 0 and ∞. At $l=1$, the effective parameters are identical with the renormalized parameters

$$u(1)=u, \quad \gamma(1)=\gamma, \quad w(1)=w, \quad F(1)=F . \tag{3.5}$$

The functions on the right-hand sides of (3.1)–(3.4) have the following form:

$$\beta_w(w,F,\gamma,u)=w[\zeta_\Gamma(w,F,\gamma,u) -\zeta_\lambda(w,F,\gamma,u)] , \tag{3.6}$$

$$\beta_F(w,F,\gamma,u)=\tfrac{1}{2}F[-\epsilon+\zeta_m(\gamma,u)-2\zeta_\lambda(w,F,\gamma,u)] , \tag{3.7}$$

$$\beta_u(u)=-\epsilon u+\tilde{\beta}_u(u) , \tag{3.8}$$

$$\beta_\gamma(\gamma,u)=\tfrac{1}{2}\gamma[-\epsilon+2\zeta_r(u)+\zeta_m(\gamma,u)] . \tag{3.9}$$

Owing to the minimal renormalization scheme, the functions ζ_Γ, ζ_λ, $\tilde{\beta}_u$, ζ_r, and ζ_m are independent of ϵ and therefore applicable directly at $\epsilon=1$ ($d=3$). The static functions β_u and ζ_r are accurately known from the Borel resummation method.[8] In the region $0\le u \lesssim O(u^*)$ these functions can be represented as[8]

$$\tilde{\beta}_u(u)=40u^2(1+15.11u)/(1+34.25u) , \tag{3.10}$$

$$\zeta_r(u)=16u(1-10u)+4851u^3-57309u^4 . \tag{3.11}$$

The function ζ_m in (3.7) and (3.9) has the form[19]

$$\zeta_m(\gamma,u)=4\gamma^2B(u) . \tag{3.12}$$

Here the u dependence is negligible,

$$B(u)=1+O(u^2) , \tag{3.13}$$

since $B(u)-1\lesssim O(\eta)$ (Ref. 41) with $\eta\simeq 0.04$ (Ref. 42).

B. Dynamic RG functions in two-loop order

To derive the function ζ_Γ up to two-loop order requires one to calculate the pole terms of the 3 one-loop and 44 two-loop diagrams that contribute to the vertex function $\mathring{\Gamma}_{\psi\tilde{\psi}^*}$, see (A1) of Appendix A. The general topology of the diagrams is shown in Fig. 1. To obtain the analytic expressions of these diagrams one must consider time-ordered vertices and distinguish between correlation and response propagators.[7,43] These expressions are given in Appendix A and the ensuing dynamic renormalization factor Z_Γ is given in Appendix C. The resulting function ζ_Γ up to $O(F^4,\gamma F^3,\gamma^2F^2,\gamma^3F,\gamma^4,\gamma Fu,F^2u,\gamma^2u,u^2)$ has the form

$$\zeta_\Gamma(w,F,\gamma,u)=\frac{4D^2}{w(1+w)}+160u^2+Q_1+Q_2-\frac{8D^4(1+2w)}{w^2(1+w)^3}\ln\left[\frac{1+2w}{(1+w)^2}\right] +4(\alpha_1+\eta_1)\ln\left[\frac{w+2w^*}{2(w+w^*)}\right]+4(\alpha_2+\eta_2+F^2D^2\delta)\ln\left[\frac{w(w+2w^*)}{(w+w^*)^2}\right], \tag{3.14}$$

with

$$D=\gamma w-\tfrac{1}{2}iF, \quad D^*=\gamma w^*+\tfrac{1}{2}iF , \tag{3.15}$$

$$\delta=\frac{2w^{*3}+3w^3+6ww^{*2}+8w^2w^*}{2w(1+w)^2w^{*3}(w+w^*)} . \tag{3.16}$$

In the following expressions for $\alpha_i(w,F,\gamma,u)$, $\eta_i(w,F,\gamma,u)$, and $Q_i(w,F,\gamma,u)$ we use the abbreviations

$$x=(1+w)^{-1}, \quad y=(w+w^*)^{-1}, \quad v=4u+2\gamma^2 . \tag{3.17}$$

The expressions read

$$\alpha_1=-2(v-i\gamma Fw^{-1})^2+8v(\gamma+\tfrac{1}{4}iF)Dx\,w^{-1}-2\gamma\,Dx^2w^{-1}[(2\gamma+iF)^2+2iF\gamma(1+w)w^{-1}] , \tag{3.18}$$

$$\eta_1=2\,D^2\gamma^2(w-w^*)xyw^{-2}+4iF\,Dx\,w^{-1}(2u+D^2x\,w^{-1}) , \tag{3.19}$$

$$\alpha_2 = -v^2 w w^{*-1} - \gamma^2 x w^{*-2}[2iF\gamma w^* + F^2(w+w^*)] + v x w^{*-2}[4\gamma^2 w w^* - iF\gamma w(2w+w^*) - \tfrac{1}{2}F^2(w+w^*)]$$
$$+2D\gamma^2 x^2[-\gamma w^{*-1} - \gamma w y + 2iF(w+w^*)w^{*-2}] , \quad (3.20)$$

$$\eta_2 = iFvxy[-D + wD^*(w+2w^*)w^{*-2}] - 2\gamma^2 D^2(w-w^*)xyw^{-2} - \tfrac{1}{2}F^2\gamma D(1+2w)x^2 y w^{-1}$$
$$+F^2\gamma D^*(w+2w^*)xyw^{*-2} - 2iFD\gamma^2 x^2 w^{*-1} + \tfrac{1}{2}\gamma F^2 D x^2 w^{*-2}[(w+2w^*)y + (w+w^*)(1-2w)w^{-1}] , \quad (3.21)$$

$$Q_1 = -16\gamma^4 w x^3(1+3w+w^2) - 8D^3x^3(\gamma + iFw^{-1}) - 8v\gamma x(\gamma w + D) + 8\gamma^3 Dx[8-(2+w)x]$$
$$-4F^2 D\gamma w x^2 y + 6\gamma F^2 D x^2 w^{*-1} - F^4 x^3 w^{-1} + 16iF\gamma^3 x(1-w^2x^2) - 4F^2\gamma^2 x^2 - 4iF^3\gamma x^3 , \quad (3.22)$$

$$Q_2 = -16(v-\gamma^2)^2 + 4(v-\gamma^2)xw^{-1}[2iF\gamma(1+2w)+F^2] + 4(v - iF\gamma w^{-1})(v+2\gamma^2+iF\gamma x)$$
$$+8vDw^{-1}(\gamma - iFx) - 32\gamma^3 D w^{-1} + 4iF\gamma^2 D x^3 - 4F^2\gamma D(1+2w)x^3 w^{-1} + iF^3 D x^2 w^{-1}(x - 3w^{*-1}) . \quad (3.23)$$

The function ζ_λ reads up to two-loop order,[11]

$$\zeta_\lambda(w,F,\gamma,u) = 4\gamma^2 - F^2 y - 2F^2 y G , \quad (3.24)$$

$$G = D^2 xy\left[\frac{1}{2} + L + \ln\left[\frac{1+w}{1+w^*}\right]\right]$$
$$+D^{*2}(1+w^*)^{-1}y\left[\frac{1}{2} + L + \ln\left[\frac{1+w^*}{1+w}\right]\right]$$
$$+2DD^*y(1+L) , \quad (3.25)$$

$$L = (w+w^*+ww^*)\ln\left[\frac{w+w^*+ww^*}{(1+w)(1+w^*)}\right] . \quad (3.26)$$

In the early work on models E and F[7,10,44–47] the dynamic coupling

$$f = \frac{g^2}{\Gamma'\lambda} = \frac{F^2}{w'} \quad (3.27)$$

was employed instead of (2.18). The corresponding β_f function is given by

$$\beta_f = 2Fw'^{-1}\beta_F - fw'^{-1}\mathrm{Re}\{\beta_w\} \quad (3.28)$$
$$= f(-\epsilon + \zeta_m - \zeta_\lambda - w'^{-1}\mathrm{Re}\{w\zeta_\Gamma\}) . \quad (3.29)$$

The last term in (3.29) corrects the last term in (3.20) of Ref. 11. Equations (3.14)–(3.23) constitute the main result of this paper.

C. Dynamic RG functions of models A, C, E

In order to check the correctness of our results (3.14)–(3.26) we have performed separate calculations of ζ_Γ and ζ_λ for models A and C (for a two-component order parameter) as well as for model E which are special cases of model F (Ref. 1). Within the minimal renormalization scheme the results in two-loop order are as follows:

Model A: $\zeta_\Gamma^A = 32u^2(-1+6\ln\tfrac{4}{3})$, $\zeta_\lambda^A = 0$. (3.30)

Model C: $$\zeta_\Gamma^C = 4\gamma^2 wx - 32u^2 + 48(2u+\gamma^2)^2\ln\tfrac{4}{3} - 96(2u+\gamma^2)\gamma^2 x\ln\tfrac{4}{3} - 64u\gamma^2 xw - 8\gamma^4 x^3 w^2$$
$$+4\gamma^4 x^2[(10+w)\ln\tfrac{4}{3} - 2w^2 x(1+2w)\ln(x^2(1+2w))] , \quad (3.31)$$

with $x = (1+w)^{-1}$, and

$$\zeta_\lambda^C = 4\gamma^2 B(u) . \quad (3.32)$$

Model E: $$\zeta_\Gamma^E = -fx + 32u^2(-1+6\ln\tfrac{4}{3}) + \tfrac{1}{4}f^2x^2(2wx - 6 + 27\ln\tfrac{4}{3}) - \tfrac{1}{2}f^2x^3(1+2w)\ln[x^2(1+2w)] , \quad (3.33)$$

$$\zeta_\lambda^E = \tfrac{1}{2}f - \tfrac{1}{8}f^2 x\{1 + 2w + 2w^2(2+w)\ln[wx^2(2+w)]\} , \quad (3.34)$$

compare Eqs. (6)–(10) of Ref. 45 for $n=2$. If one takes the appropriate limits of the model-F results (3.14)–(3.26) one indeed finds agreement with (3.30)–(3.34). The corresponding limiting cases are $\gamma = F = 0$ and $w''=0$ for model A, $F=0$ and $w''=0$ for model C, and $\gamma=0$ and $w''=0$ for model E. This guarantees the correctness at least of the terms of $O(F^2,\gamma^2,F^4,\gamma^4,\gamma^2 u,u^2)$ for $w''=0$ in (3.14)–(3.26). We have of course checked the whole calculation several times also with respect to all other terms.

D. Fixed point

In the early analysis[7,44–47] of the possible instability of the dynamic-scaling fixed point the static fixed-point value u^* was taken into account only in the one-loop form $u^* = \epsilon/40$ which is rather inaccurate at $\epsilon = 1$. In this subsection we update this analysis on the basis of the more accurate knowledge of u^* according to the Borel resummation result (3.10). The justification of using this

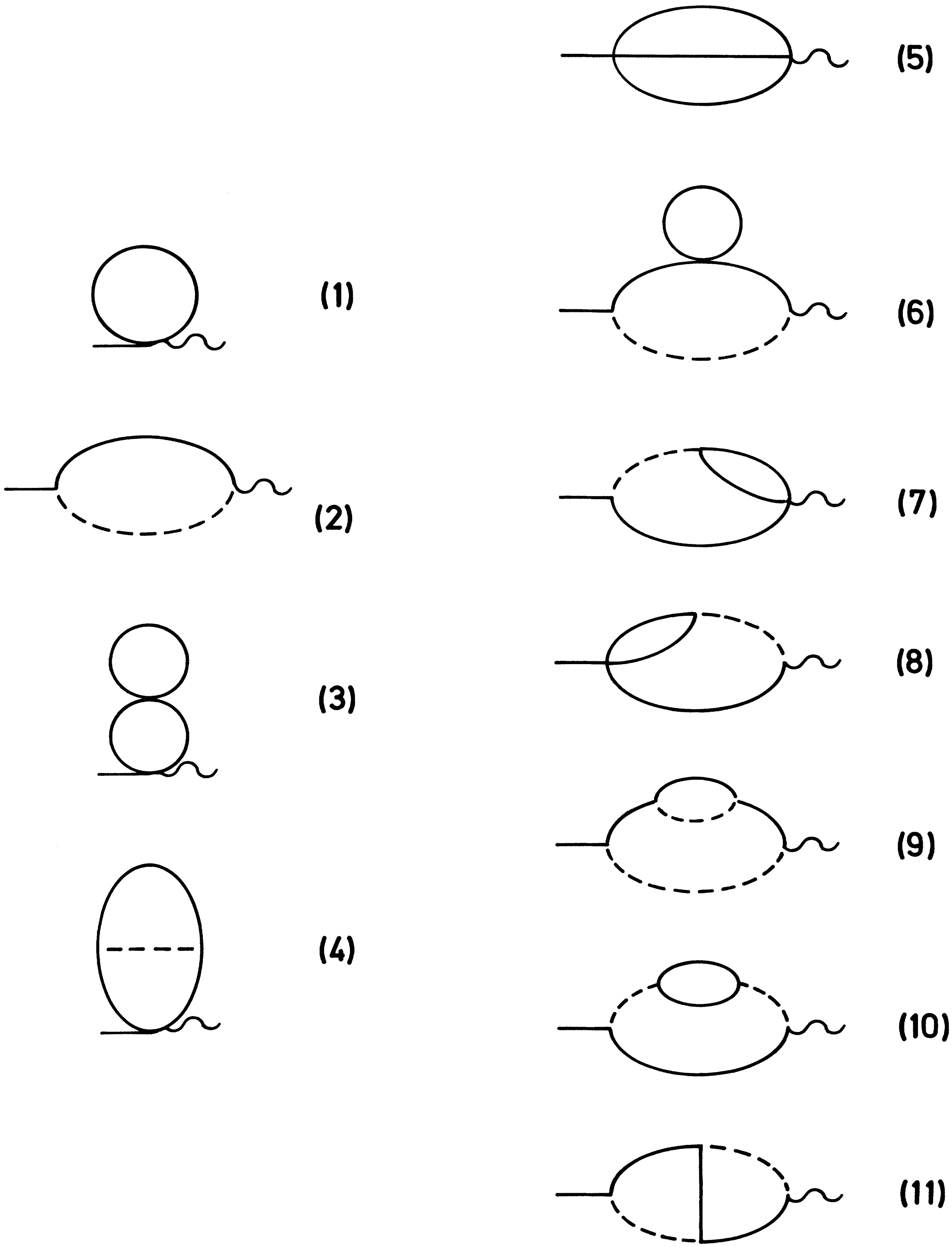

FIG. 1. Topology of one- and two-loop diagrams that contribute to the vertex function $\mathring{\Gamma}_{\psi\tilde{\psi}*}$ and determine the function ζ_Γ, (2.23), (3.14). The solid and dashed internal lines indicate propagators of the order parameters ψ_0 and of the entropy variable m_0, respectively, without distinguishing between correlation and response propagators. The analytic expressions at $k=0$ are given in Appendix A.

value within our two-loop calculation will be given at the end of this subsection. In Fig. 2 we have plotted $u^*(\epsilon)$ as obtained from (3.8) and (3.10), $\epsilon u^* = \tilde{\beta}_u(u^*)$.

In the following we first consider model E (with $\gamma=0$, $w''=0$). The borderline dimension $d^*=4-\epsilon^*$ below which the dynamic-scaling fixed point is unstable is determined by the three conditions[44]

$$(w')^*=0 \ , \tag{3.35}$$

$$\zeta_\lambda^* = \zeta_\Gamma^* \ , \tag{3.36}$$

$$0=\epsilon^* + \zeta_\lambda^* + \zeta_\Gamma^* \ . \tag{3.37}$$

Eliminating ζ_Γ^* from (3.36) and (3.37) and using the two-loop result (3.34) yields

$$f^* = 2[(1+\epsilon^*)^{1/2} - 1] \tag{3.38}$$

at the borderline dimension. Equations (3.33), (3.34), (3.36), and (3.38) lead to the following relation between ϵ^* and $u^*(\epsilon^*)$:

$$32(-1+6\ln\tfrac{4}{3})u^*(\epsilon^*)^2 = (1+\epsilon^*)^{1/2} - 1 - (-\tfrac{11}{2} + 27\ln\tfrac{4}{3})[(1+\epsilon^*)^{1/2}-1]^2 \ . \tag{3.39}$$

Together with the known function $u^*(\epsilon)$, Fig. 2, this determines ϵ^* as

$$\epsilon^* = 0.986, \quad d^* = 3.014 \ . \tag{3.40}$$

Thus we conclude that, within the present approximation, the dynamic-scaling fixed point is unstable for $d<3.014$ and the weak-scaling fixed point[7] with $(w')^*=0$ is stable in three dimensions. This statement remains valid also for model F which has the same (stable) fixed point as model E in three dimensions because of

$$(w'')^*=0 \tag{3.41}$$

and

$$\gamma^*=0 \ . \tag{3.42}$$

Equation (3.42) follows from (3.9) since $\alpha/\nu = 1-2\zeta_r(u^*)$ is negative in three dimensions.[42] From $\beta_f=0$ we calculate the fixed-point value of f in three dimensions

$$f^* = 0.834 \ , \tag{3.43}$$

where we have used[8,48]

$$u^* = 0.0362 \ . \tag{3.44}$$

Equations (3.35) and (3.43) imply

$$F^* = [f^*(w')^*]^{1/2} = 0 \ . \tag{3.45}$$

In summary, the stable fixed point of model F at $d=3$ in two-loop order (with the Borel-resummed static fixed-point value u^*) is described by Eqs. (3.35), (3.41)–(3.45). For the transient exponent $\omega_w = \zeta_\Gamma^* - \zeta_\lambda^*$ we find in three dimensions

$$\omega_w = 0.008 \ . \tag{3.46}$$

Finally we comment on our use of the Borel sum value of u^* in the expression for ζ_Γ^E which is only of order-two loops. The effect of u^* on the dynamic-fixed point enters through the second term of Eq. (3.33) which is identical with the model A part, Eq. (3.30),

$$\zeta_\Gamma^A(u^*) = 32u^{*2}(-1+6\ln\tfrac{4}{3}) \ . \tag{3.47}$$

It is known[1,7] that Eq. (3.47) gives the two-loop approximation for the dynamic critical exponent z_A of model A,

$$z_A - 2 = \zeta_\Gamma^A(u^*) = c\eta \ , \tag{3.48}$$

where η is the well-known static critical exponent (for $n=2$)

$$\eta = 32u^{*2} + O(u^{*3}) \ . \tag{3.49}$$

If (in the spirit of the ϵ expansion) the value $u^*=\epsilon/40$ is used in the two-loop result (3.49) one obtains $\eta=0.020$ at $\epsilon=1$, in clear disagreement with the Borel sum value $\eta=0.038$ in three dimensions.[8] By contrast, if we use the Borel sum value[8] $u^*=0.0362$ in the two-loop result (3.49) we obtain $\eta=0.0419$ in close agreement with the correct value of η. For this reason we believe that the use of $u^*=0.0362$ is also justified in (3.47) and in $\zeta_\Gamma^E(u^*)$. Clearly our results do not yet definitely establish the instability of the dynamic-scaling fixed point at $d=3$ because the *dynamic* higher-loop contributions may change the value of d^*. For further discussions see Refs. 2, 3, 44–47.

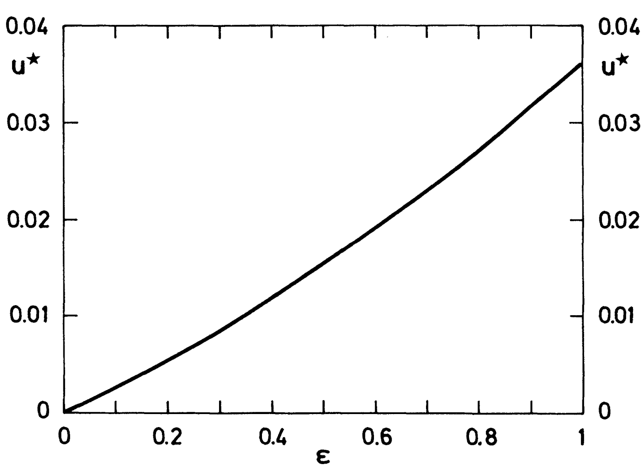

FIG. 2. Fixed point value u^* as a function of $\epsilon=4-d$ as obtained from $\epsilon u^* = \tilde{\beta}_u(u^*)$ with $\tilde{\beta}_u(u)$ given by (3.10). At $\epsilon=1$, $u^*=0.0362$.

IV. EFFECTIVE RENORMALIZED PARAMETERS FOR THE λ TRANSITION

In this section we describe the procedure how to determine the nonuniversal effective renormalized parameters $u(l)$, $\gamma(l)$, $w(l)$, $F(l)$ for the λ transition of ^{4}He at several pressures. The present model-F analysis differs from the previous ones[23,24] in that here we employ the more accurate Borel-resummation results[8] for $\beta_u(u)$, $\zeta_r(u)$, and for the amplitude function[19,49] $F_+(u)$ of the specific heat. We choose the flow parameter $l=l(t)$ above T_λ by requiring

$$\frac{r(l)}{\mu^2 l^2}=1, \quad \mu=\xi_0^{-1} \tag{4.1}$$

where[19]

$$r(l)=r(1)\exp\int_1^l \zeta_r(u(l'))\frac{dl'}{l'} . \tag{4.2}$$

$$r(1)=at, \quad t=\frac{T-T_\lambda(P)}{T_\lambda(P)}>0 , \tag{4.3}$$

and[9]

$$a=\xi_0^{-2}Q^*\exp\int_u^{u^*}\frac{\zeta_r(u^*)-\zeta_r(u')}{\beta_u(u')}du' \tag{4.4}$$

with $Q^*=Q(1,u^*,3)=0.939$ in three dimensions.[49] The nonuniversal constant (4.4) will not enter the following analysis since we shall need only[19]

$$\frac{t}{l}\frac{dl(t)}{dt}=[2-\zeta_r(u(l(t)))]^{-1} . \tag{4.5}$$

A. Effective static couplings

We wish to identify the effective static couplings

$$u[t]\equiv u(l(t)), \quad \gamma[t]\equiv\gamma(l(t)) , \tag{4.6}$$

as a function of the reduced temperature $t>0$. According to (3.3), (3.4), and (4.5) the RG flow equations for $u[t]$ and $\gamma[t]$ read

$$t\frac{du[t]}{dt}=\frac{\beta_u(u[t])}{2-\zeta_r(u[t])} . \tag{4.7}$$

$$t\frac{d\gamma[t]}{dt}=\frac{\beta_\gamma(\gamma[t],u[t])}{2-\zeta_r(u[t])} . \tag{4.8}$$

The information on the nonuniversal initial values $u[t_0]$ and $\gamma[t_0]$ at some convenient t_0 can be extracted from the logarithmic derivative of the measured specific heat $\mathring{C}(t)$ above T_λ. In terms of the minimally renormalized theory in three dimensions the logarithmic derivative of the specific heat is represented as[19]

$$\frac{t}{\mathring{C}(t)}\frac{d\mathring{C}(t)}{dt} =(\gamma[t])^2\frac{(2\zeta_r-1)F_+-4+\beta_u\partial F_+/\partial u}{(2-\zeta_r)[1+\gamma[t]^2F_+]}, \tag{4.9}$$

where the functions F_+, ζ_r, and β_u on the right-hand side (RHS) have the arguments $F_+(u[t])$, $\zeta_r(u[t])$, and $\beta_u(u[t])$. Equation (4.9) is an approximation in the sense that finite-cutoff effects are neglected. Furthermore we have used $B=1$, see (3.13). The function $F_+(u)$ is given by[49]

$$F_+(u)=-2-16u(1+7.59u) \tag{4.10}$$

(a comment on this function will be given at the end of this subsection). For the experimental specific heat $C_p=k_B\mathring{C}(t)$ we employ the representation (3a)–(3f) of Tam and Ahlers[24]

$$k_B\mathring{C}(t)=A[(1/\alpha)(t^\alpha-1)+\tilde{D}t^{\Delta-\alpha}+\tilde{B}] . \tag{4.11}$$

The parameters A, $\tilde{D}$, and $\tilde{B}$ depend on t and on the pressure.[24,50] In order to ensure precise consistency of the theoretical expressions (4.7)–(4.9) with the experimental values[24] for α and ν one should use $2-\zeta_r$ and $2\zeta_r-1$ in the forms

$$2-\zeta_r(u)=\nu^{-1}+\zeta_r(u^*)-\zeta_r(u) \tag{4.12}$$

and

$$2\zeta_r(u)-1=-\frac{\alpha}{\nu}+2[\zeta_r(u)-\zeta_r(u^*)] , \tag{4.13}$$

with $\alpha=-0.016$ and $\nu=0.672$. Thus the Borel-resummation result (3.11) for $\zeta_r(u)$ will be used in (4.7)–(4.9) only in the form of the difference $\zeta_r(u)-\zeta_r(u^*)$, with $u^*=0.0362$. This procedure can be easily applied also to the specific heat data of Chui and Lipa[51] with slightly different values for α and ν. For β_u and β_γ in (4.7)–(4.9) we used (3.8)–(3.13) with $\epsilon=1$. In (3.9) the substitution (4.13) is to be made as well.

The final step is to determine the appropriate solutions $u[t]$ and $\gamma[t]$ of (4.7) and (4.8) by adjusting the initial values $u[t_0]$ and $\gamma[t_0]$ at some convenient t_0 such that the RHS of (4.9) agrees with the (experimentally determined) LHS of (4.9) over some range of t, i.e., one has to perform a least-squares fit with two adjustable parameters. We have chosen $t_0=10^{-3}$. The initial values are given in Table I for several pressures. The corresponding effective parameters $u[t]$ and $\gamma[t]$ as obtained by numerical integration of (4.7) and (4.8) are plotted in Fig. 3 for *SVP* and $P=28$ bars. They are very close to those plotted in Fig. 2 of Ref. 52 but differ from those of Refs. 24 and 29 by about 10%. This difference is mainly due to the approximations with regard to β_u, ζ_r, and F_+ that have been employed in Ref. 19 on which the analysis of Refs. 24 and 29 was based. For the range $t>10^{-3}$ the parameter $\gamma[t]$ should be replaced by the phenomenological parameter $\gamma[t]^{\text{expt}}$, see Appendix D. This parameter is also plotted in Fig. 3.

The procedure described above is only one possible way among several equivalent procedures of determining $u[t]$ and $\gamma[t]$. A general discussion of determining the nonuniversal parameters of the theory including finite-cutoff effects will be given elsewhere.[53] Here we only note that the cutoff effects may be non-negligible in determining the sign and magnitude of the leading correction amplitudes and in determining the asymptotic value of $\mathring{C}$ at T_λ. In a theory that neglects finite-cutoff effects (in particular in our minimally renormalized theory) some apparently unusual features may arise such as formally negative values of $\gamma[t]^2$ for large t and positive values of $u[t]-u^*$. This will be of relevance in a reexamination of the analysis of the specific heat of ^{4}He performed by Bagnuls and Bervillier[54] and in a field-theoretic description of the results found by Liu and Fisher[55] for the sign of the correction amplitudes of the three-dimensional Ising

TABLE I. Initial values $u[t_0]$, $\gamma[t_0]$, $w[t_0]$, $F[t_0]$ at $t_0=10^{-3}$ of the RG flow equations (4.7), (4.8), (4.17), and (4.18) of model *F*. The static parameters $u[t_0]$ and $\gamma[t_0]$ are determined from fits to the experimental specific heat (Refs. 24 and 50) according to (4.9) and (4.11), the dynamic parameters are derived from fits of $R_\lambda^{\rm theor}(t)$, (4.25), to the data of Ref. 50 in the range $10^{-6}<t\leq 10^{-3}$. The corresponding effective parameters $w'[t]$, $w''[t]$, and $f[t]$ as well as $R_\lambda^{\rm theor}$ are plotted in Fig. 4 for *SVP* (0.05 bars) and 28 bars. See also Ref. 56 for numerical values and for intermediate pressures.

P (bars)	$u[t_0=10^{-3}]$	$\gamma[t_0=10^{-3}]$	$w'[t_0=10^{-3}]$	$w''[t_0=10^{-3}]$	$F[t_0=10^{-3}]$
SVP	0.035 77	0.2395	0.5962	0.5681	0.7949
6.85	0.035 47	0.2476	0.7040	0.5317	0.8242
14.73	0.034 89	0.2589	0.8106	1.0452	0.8352
22.30	0.033 69	0.2657	0.9549	0.8909	0.8310
28.00	0.033 07	0.2844	1.0431	0.6819	0.7998

model.

Finally we comment on the function (4.10). In the context of Eq. (4.1) and (4.9) this function is identical with $F_+[u,1]$ defined in (4.6) of Ref. 19 and should, in principle, be distinguished from $F_+(1,u,3)$ of Refs. 9 and 49 where the flow parameter was chosen differently. The connection between these functions is[9]

$$F_+[u,Q(1,u,3)]=F_+(1,u,3)\ , \tag{4.14}$$

where $Q(1,u,3)$ is the amplitude function of the correlation length.[8] It is this function (4.14) that has been computed in Ref. 49 by means of Borel resummation rather than $F_+[u,1]$. The latter is not Borel resummable due to $\ln u$ terms. One can verify, however, that the difference between $F_+[u,1]$ and $F_+[u,Q(1,u,3)]$ is less than 0.1% in the range $0\leq u\leq u^*$ and that therefore the representation (4.10), with the same coefficient[49] $b_F=7.59$ as computed for $F_+(1,u,3)$, is justified within the present error bars. This comment applies in particular to the fixed-point value $F_+[u^*,1]$ since

$$F_+[u^*,1],=Q(1,u^*,3)^\alpha F_+(1,u^*,3)$$
$$\approx F_+(1,u^*,3)\ . \tag{4.15}$$

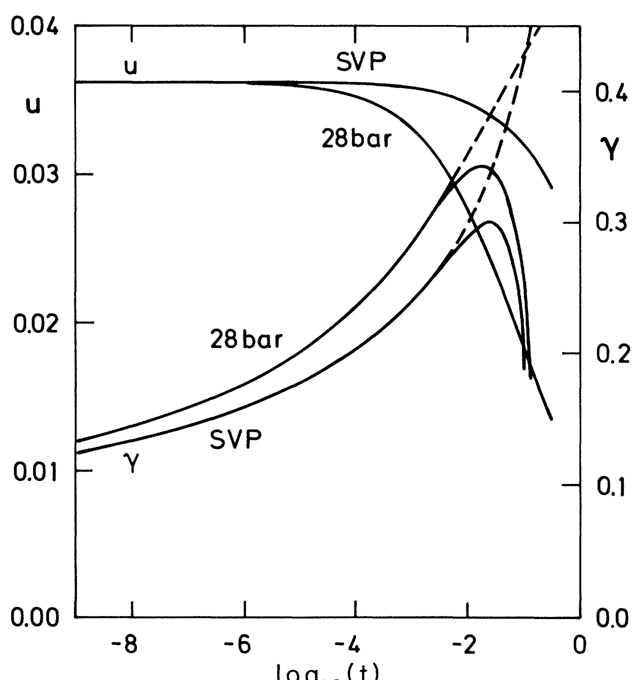

FIG. 3. Effective static parameters $u[t]$, $\gamma[t]$, and $(\gamma[t])^{\rm expt}$ for *SVP* and 28 bar. $u[t]$ is obtained by integrating Eq. (4.7) with the initial values of $u[10^{-3}]$ given in Table I. $(\gamma[t])^{\rm expt}$ (solid lines) is obtained from Eq. (D2). For $t\leq 10^{-3}$, $(\gamma[t])^{\rm expt}$ is essentially identical with the solution $\gamma[t]$ of the RG flow equation (4.8) with the initial values $\gamma[10^{-3}]$ given in Table I. For $t>10^{-3}$, $\gamma[t]$ (dashed lines) differs significantly from $(\gamma[t])^{\rm expt}$ (solid lines). For intermediate pressures and for numerical values of $u[t]$, $\gamma[t]$, and $(\gamma[t])^{\rm expt}$ see Table II and Ref. 56.

B. Effective dynamic parameters

In this subsection we describe how to determine the effective dynamic parameters

$$w[t]=w(l(t)),\quad F[t]=F(l(t))\ , \tag{4.16}$$

on the basis of the two-loop model-*F* RG flow equations for the λ transition of ^{4}He. The resulting $w[t]$ and $F[t]$ are more accurate than those of the earlier model-*F* analyses[11,23,24] in that we take into account the Borel resummation results for the static functions $\beta_u(u)$, $\zeta_r(u)$, and $F_+(u)$. The parameters (4.16) satisfy the RG flow equations

$$t\frac{dw[t]}{dt}=\frac{\beta_w(w[t],F[t],\gamma[t],u[t])}{2-\zeta_r(u[t])}\ , \tag{4.17}$$

$$t\frac{dF[t]}{dt}=\frac{\beta_F(w[t],F[t],\gamma[t],u[t])}{2-\zeta_r(u[t])}\ , \tag{4.18}$$

where the known effective static couplings $\gamma[t]$ and $u[t]$ of Sec. IV A and Appendix D have to be inserted. For the denominator $2-\zeta_r$ the substitution (4.12) should be made. The nonuniversal initial values $w[t_0]$ and $F[t_0]$ of (4.17) and (4.18) can be determined[47] from a least-squares fit to the thermal conductivity data.

Within model F, the theoretical expression for the thermal conductivity λ_T can be derived from the (bare) vertex function $\mathring{\Gamma}_{m\tilde{m}}(k,\omega)$ at $\omega=0$ according to[11]

$$\lambda_T = C_P \frac{\partial}{\partial k^2} \mathring{\Gamma}_{m\tilde{m}}(k,0)\Big|_{k=0} , \tag{4.19}$$

where $C_P = k_B \mathring{C}$ is the (bare) constant-pressure specific heat per unit volume. Neglecting finite-cutoff effects we rewrite the RHS of (4.19) in terms of renormalized quantities as[11,19]

$$\lambda_T = k_B Z_m(\gamma,u)\chi_o \lambda[1+fP(w,F,\gamma,u,r/\mu^2)] \tag{4.20}$$

$$= k_B Z_m(\gamma,u)\chi_0\lambda(l)[1+f(l)P(w(l),F(l),\gamma(l),u(l),1)] \times \exp\int_l^1 \zeta_m \frac{dl'}{l'} \tag{4.21}$$

$$= g_0(\mu l)^{-\epsilon/2} k_B^{1/2} C_P^{1/2} R_\lambda^{\text{eff}}(w(l),F(l),\gamma(l),u(l)) \tag{4.22}$$

with

$$R_\lambda^{\text{eff}}(w,F,\gamma,u) = \frac{A_d^{1/2}[1+fP(w,F,\gamma,u,1)]}{F[1+\gamma^2 F_+(u)]^{1/2}} . \tag{4.23}$$

In (4.21) and (4.22) the flow parameter is chosen according to (4.1). In three dimensions R_λ^{eff} becomes

$$R_\lambda^{\text{eff}}(w,F,\gamma,u) = \frac{1-f/4+fM_3(w,F,\gamma)}{2\pi^{1/2}F[1+\gamma^2 F_+(u)]^{1/2}} \tag{4.24}$$

with $F_+(u)$ given by (4.10) and with $M_3(w,F,\gamma)$ given by (4.13)–(4.17) of Ref. 11 (up to two-loop order). The theoretical quantity to be compared with the experimental data is

$$R_\lambda^{\text{theor}}(t) \equiv R_\lambda^{\text{eff}}(w[t],F[t],\gamma[t],u[t]) . \tag{4.25}$$

The experimental counterpart of $R_\lambda^{\text{theor}}(t)$ is

$$R_\lambda^{\text{expt}}(t) = \lambda_T(t) g_0^{-1}[\xi(t) k_B C_P(t)]^{-1/2} , \tag{4.26}$$

where $\lambda_T(t)$, $C_P(t)$, and $\xi(t)$ are the measured thermal conductivity, specific heat, and correlation length, respectively. For the experimental values of these quantities and of g_0 see Refs. 24 and 50. Now we are in the position to perform least-squares fits of $R_\lambda^{\text{theor}}(t)$ to $R_\lambda^{\text{expt}}(t)$ with three adjustable parameters $w[t_0]=w'[t_0]+iw''[t_0]$ and $F[t_0]$. For $R_\lambda^{\text{expt}}(t)$ we use the thermal-conductivity data of cell F (Ref. 50).

The initial values at $t_0=10^{-3}$ are given in Table I for several pressures. The resulting effective parameters $w'[t]$, $w''[t]$, and $f[t]=(F[t]^2)/w'[t]$, as obtained by numerical integration of (4.17) and (4.18), are shown in Fig. 4 in the range $10^{-9} \le t \le 10^{-3}$ for SVP and 28 bar. Numerical values for the effective parameters are presented in Ref. 56 which also includes the case of intermediate pressures $P=6.85$, 14.73, 22.30 bars.

It should be noted that in comparing (4.25) with (4.26) we have made the approximation $(\mu l)^{-1/2} \approx \xi^{1/2}$. Here we have neglected a factor $[Q(1,u,(l),3)]^{1/2}$. This factor is close to 1, see Fig. 2 of Ref. 49, thus the approximation $Q^{1/2} \approx 1$ is well justified within the error bars of our two-loop approximation for R_λ^{eff}.

In Fig. 4 we also present the prediction for R_λ^{eff} very close to T_λ for SVP and 28 bars as calculated from the effective parameters $w[t]$,$F[t]$, $\gamma[t]$,$u[t]$. (Compare Fig. 3 of Ref. 23 and Fig. 7 of Ref. 24.) If the dynamic-scaling prediction[57] and the corresponding one-loop RG result[10] were valid the amplitude R_λ^{eff} would become a *universal constant*[10] for $t \lesssim 10^{-3}$. By contrast, our theory implies significant deviations from dynamic scaling, namely, a monotonic increase of R_λ^{eff} as T_λ is approached, in accord with the original prediction in Fig. 4 of Ref. 47. This is in qualitative disagreement with the nonmonotonic behavior of the data of Lipa and Chui.[27]

The asymptotic behavior of R_λ^{eff} is in two-loop order[11]

$$R_\lambda^{\text{eff}} \sim \frac{1-f^*/4-f^{*2}/8}{2\pi^{1/2}(f^*)^{1/2}[w'(l)]^{1/2}} , \tag{4.27}$$

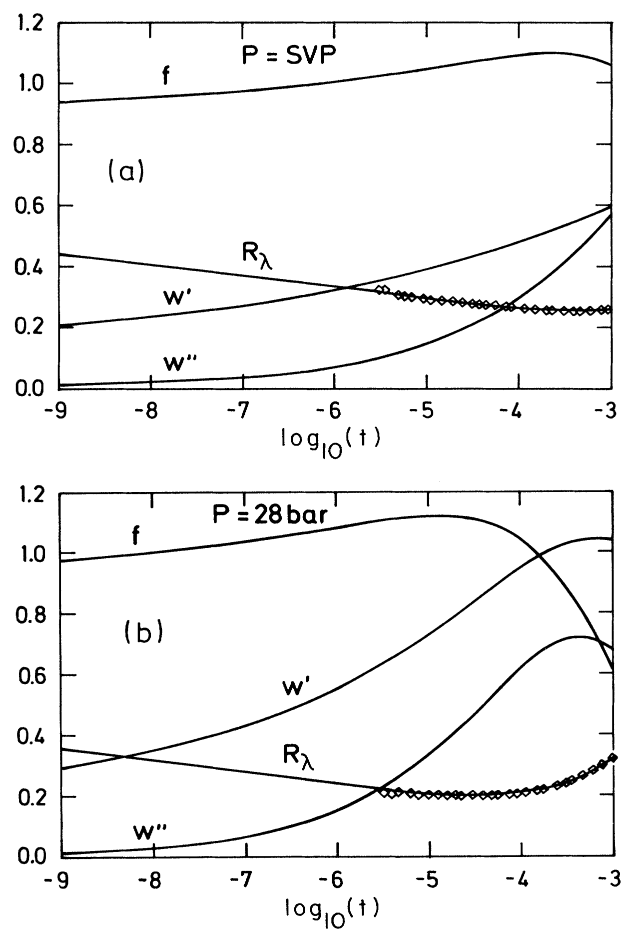

FIG. 4. Effective parameters $w'[t]$, $w''[t]$, and $f[t]$ of model F as obtained by integrating the RG flow equations (4.7), (4.8), (4.17), and (4.18) with the initial values given in Table I. The resulting effective amplitude $R_\lambda^{\text{theor}}(t)$, (4.25), is also shown. The data are taken from Ref. 50. (a) SVP, (b) 28 bars. For intermediate pressure and for numerical values of the effective parameters see Ref. 56.

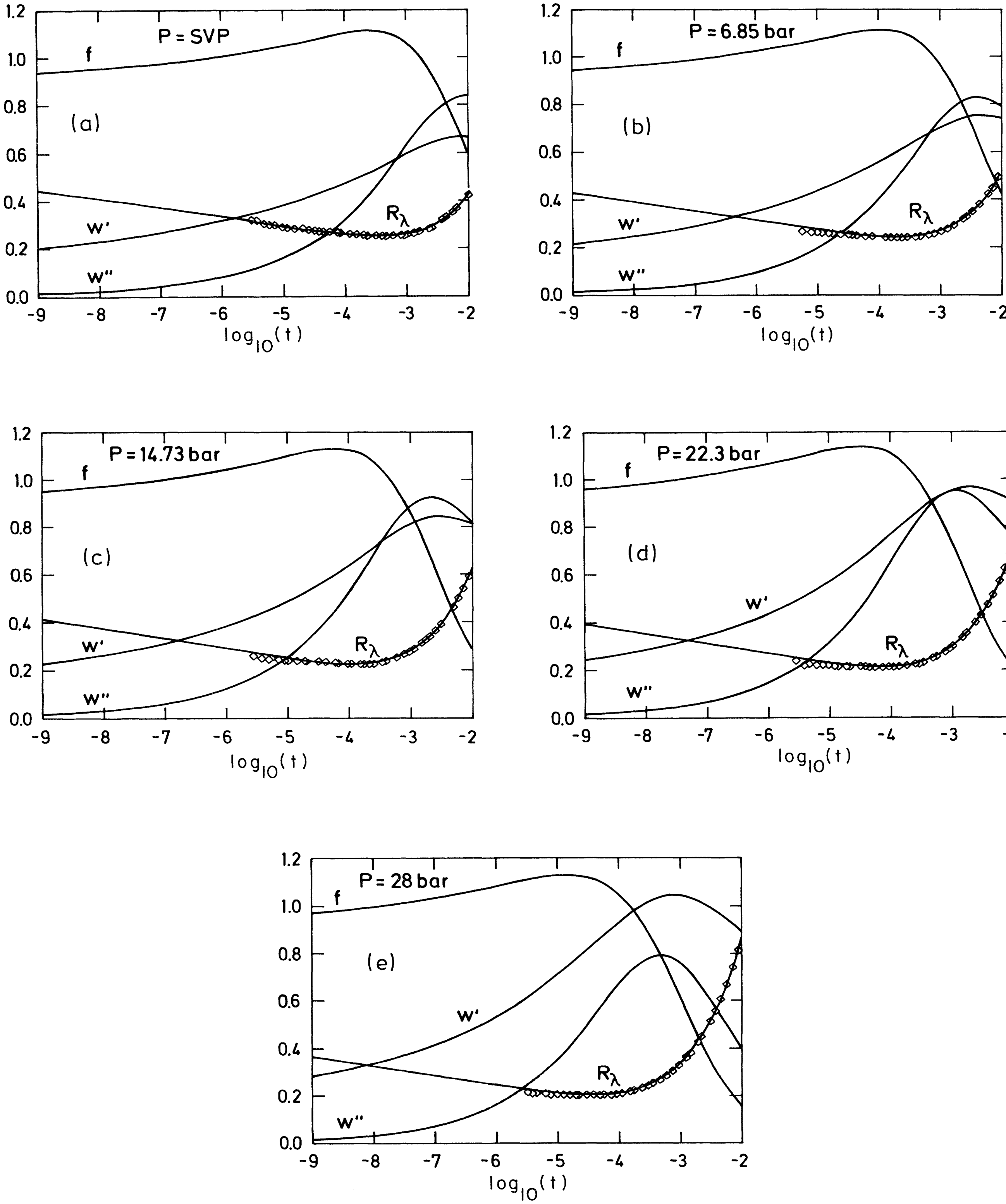

FIG. 5. Effective parameters $w'[t]$, $w''[t]$, and $f[t]=(F[t])^2/w'[t]$ of model F as obtained by integrating (4.17) and (4.18) and by fitting $R_\lambda^{\text{theor}}(t)$, (4.25), to the data of Ref. 50 in the range $10^{-6}<t\le 10^{-2}$. (a) *SVP*, (b) 6.85 bars, (c) 14.73 bars, (d) 22.3 bars, (e) 28.0 bars. The static coupling $u[t]$ employed in this fit is the solution of the RG flow equation (4.7) with the initial values $u[t_0=10^{-3}]$ of Table I. Instead of the solution $\gamma[t]$ of (4.8) the effective coupling $(\gamma[t])^{\text{expt}}$ is employed which is derived from Eq. (D2). For numerical values see Table II and Ref. 56.

TABLE II. Representative values of the effective parameters $u[t]$, $(\gamma[t])^{\text{expt}}$, $w[t]$, and $F[t]$ as well as $R_\lambda^{\text{theor}}(t)$ for *SVP* (0.05 bars) and 28 bars. $u[t]$ is obtained by integrating Eq. (4.7) with the initial values $u[t_0=10^{-3}]$ given in Table I. $(\gamma[t])^{\text{expt}}$ is determined from Eq. (D2). The dynamic parameters $w'[t]$, $w''[t]$, and $F[t]$ are the solutions of (4.17) and (4.18) with initial values that are determined from fits of $R_\lambda^{\text{theor}}(t)$, (4.25), to the data of Ref. 50 in the range $10^{-6}<t\leq 10^{-2}$. The effective parameters and R_λ^{theor} are plotted in Figs. 3 and 5. See also Ref. 56 for additional numerical values and for intermediate pressures.

P (bars)	$-\log_{10}t$	$u[t]$	$(\gamma[t])^{\text{expt}}$	$w'[t]$	$w''[t]$	$F[t]$	$R_\lambda^{\text{theor}}(t)$
SVP	1.0	0.031 81	0.2070				
SVP	2.0	0.034 78	0.2887	0.6699	0.8325	0.6306	0.4294
SVP	3.0	0.035 77	0.2393	0.5955	0.6320	0.7954	0.2624
SVP	4.0	0.036 07	0.2034	0.4751	0.3263	0.7241	0.2637
SVP	6.0	0.036 19	0.1606	0.3168	0.0808	0.5648	0.3373
SVP	9.0	0.036 20	0.1261	0.2021	0.0129	0.4351	0.4442
28	1.0	0.018 00	0.2535				
28	2.0	0.027 52	0.3378	0.8938	0.4024	0.3798	0.8464
28	3.0	0.033 07	0.2842	1.0452	0.7590	0.7999	0.3324
28	4.0	0.035 22	0.2361	0.9290	0.6638	0.9895	0.2109
28	6.0	0.036 11	0.1784	0.5331	0.1640	0.7605	0.2460
28	9.0	0.036 19	0.1354	0.2830	0.0156	0.5242	0.3646

where

$$w'(l)=a_w\xi^{-\omega_w}+O(\xi^{-2\omega_w}),\quad \xi\sim\xi_0 t^{-\nu}\ , \tag{4.28}$$

with a nonuniversal (pressure-dependent) amplitude a_w and with ω_w given by (3.46). Thus R_λ^{eff} is predicted to diverge (weakly) if the weak-scaling fixed point[7] $(w')^*=0$ is stable. Because of $\omega_w \ll 1$, however, the pure power-law behavior $\sim ct^{-\nu\omega_w/2}$ of R_λ^{eff} is unobservable, as discussed in Refs. 47 and 58.

Finally we present the results for the effective dynamic parameters on the basis of fits with $t_0=10^{-2}$ which include the thermal conductivity data in the range $t\leq 10^{-2}$. In this range $\gamma[t]$ is replaced by $(\gamma[t])^{\text{expt}}$, as described in Appendix D. The resulting dynamic parameters as well as $R_\lambda^{\text{theor}}(t)$ are shown in Fig. 5. We consider these parameters, together with $u[t]$ and $(\gamma[t])^{\text{expt}}$ of Fig. 3, as the "standard parameters" of model F. For numerical values see Table II and Ref. 56. These parameters can be applied to other critical phenomena above and below the λ line provided that the flow parameter (1.3) is employed appropriately.

Note added in proof. Measurements of the thermal conductivity at SVP in the range $10^{-7}\leq t\leq 10^{-3}$ have been reported recently by J. A. Lipa (unpublished). The data show a monotonic increase of R_λ as T_λ is approached, in agreement with the predictions of this paper [Figs. 4(a) and 5(a)].

ACKNOWLEDGMENTS

I am grateful to G. Moser and P. Sutter for carrying out the numerical computation of the effective parameters of Tables I and II, and of Figs. 3–5.

APPENDIX A: DYNAMIC PERTURBATION CALCULATION

The perturbation calculation is based on the dynamic functional[59,60] given in (A2)–(A9) of Ref. 11. The unrenormalized vertex functions of interest are $\mathring{\Gamma}_{m\tilde{m}}$ and $\mathring{\Gamma}_{\psi\tilde{\psi}^*}$. The two-loop expression for $\mathring{\Gamma}_{m\tilde{m}}$ has already been given in Refs. 11 and 61 at arbitrary wave number k and arbitrary frequency ω. In this Appendix we shall present the two-loop expression for $\mathring{\Gamma}_{\psi\tilde{\psi}^*}(\omega)$ at $k=0$ and arbitrary ω:

$$\mathring{\Gamma}_{\psi\tilde{\psi}^*}(\omega)=\tfrac{1}{2}(-i\omega+\Gamma_0\tau_0+ig_0h_0)-\sum_{\nu=1}^{11}X_\nu(\omega)\ . \tag{A1}$$

The one- and two-loop contributions $X_\nu(\omega)$ come from the diagrams of the type $\nu=1,2,\ldots,11$ shown in Fig. 1. To obtain the analytic expressions of these diagrams one must consider time-ordered vertices and distinguish between correlation and response propagators. The number N_ν of different time-ordered diagrams of each type ν shown in Fig. 1 is as follows. *One-loop diagrams:* $N_1=1$, $N_2=2$. *Two-loop diagrams:* $N_3=2$, $N_4=5$, $N_5=2$, $N_6=3$, $N_7=5$, $N_8=5$, $N_9=7$, $N_{10}=7$, $N_{11}=8$.

We shall use the notations

$$\int_p \equiv (2\pi)^{-d}\int d^dp\ , \tag{A2}$$

$$J_N(\tau_0)=\int_p (p^2+\tau_0)^{-N},\quad N=1,2\ , \tag{A3}$$

$$a_3=\lambda_0\chi_0^{-1}\gamma_0+\tfrac{1}{2}ig_0\chi_0^{-1}\ , \tag{A4}$$

$$b_3=\Gamma_0\gamma_0-\tfrac{1}{2}ig_0\chi_0^{-1}\ , \tag{A5}$$

$$b_4=2\Gamma_0\tilde{u}_0-\tfrac{1}{2}ig_0\gamma_0\ , \tag{A6}$$

$$\pi_n=p_n^2+\tau_0,\quad n=1,2,\quad \pi_{12}=(\mathbf{p}_1+\mathbf{p}_2)^2+\tau_0\ , \tag{A7}$$

$$K_n=\Gamma_0\pi_n+\lambda_0\chi_0^{-1}p_n^2,\quad n=1,2\ , \tag{A8}$$

$$L_n=\gamma_0K_n-\tfrac{1}{2}i\tau_0g_0\chi_0^{-1},\quad n=1,2\ , \tag{A9}$$

$$K_{12}=\Gamma_0\pi_{12}+\lambda_0\chi_0^{-1}(p_1^2+p_2^2)\ , \tag{A10}$$

$$L_{12}=\gamma_0K_{12}-\tfrac{1}{2}i\tau_0g_0\chi_0^{-1}\ , \tag{A11}$$

$$G_{12}=\Gamma_0(\pi_1+\pi_2)+\Gamma_0^*\pi_{12}\ , \tag{A12}$$

$$A_{12}=\gamma_0\lambda_0\chi_0^{-1}p_1^2+\tfrac{1}{2}ig_0\chi_0^{-1}(\pi_{12}-\pi_2)\ . \tag{A13}$$

The analytic expressions for the sum of the N_ν diagrams of the type ν read

$$X_1=-4b_4J_1(\tau_0)\ , \tag{A14}$$

$$X_2=2b_3\chi_0\int_{p_1}\frac{L_1}{\pi_1(K_1+ig_0h_0-i\omega)}\ , \tag{A15}$$

$$X_3=64\tilde{u}_0b_4J_1(\tau_0)J_2(\tau_0)\ , \tag{A16}$$

$$X_4=-16\gamma_0^2\chi_0b_4J_1(\tau_0)J_2(\tau_0)\ , \tag{A17}$$

$$X_5=16b_4\int_{p_1}\int_{p_2}\frac{2b_4\pi_1+b_4^*\pi_{12}}{\pi_1\pi_2\pi_{12}(G_{12}-i\omega)}\ , \tag{A18}$$

$$X_6=\int_{p_1}\int_{p_2}\frac{-16b_3\chi_0}{\pi_1^2\pi_2(K_1-i\omega)}\left[2\tilde{u}_0a_3p_1^2+\frac{b_4L_1\pi_1}{K_1-i\omega}\right]\ , \tag{A19}$$

$$X_7=\int_{p_1}\int_{p_2}\frac{-16b_4\chi_0}{\pi_1\pi_2\pi_{12}(G_{12}-i\omega)}\left[b_3\gamma_0\pi_1+\frac{L_1(b_3\pi_2+b_3^*\pi_{12})}{K_1-i\omega}\right]\ , \tag{A20}$$

$$X_8=\int_{p_1}\int_{p_2}\frac{-16b_3\chi_0}{\pi_1\pi_2\pi_{12}(K_1-i\omega)}\left[b_4\gamma_0\pi_1+\frac{A_{12}[b_4(\pi_1+\pi_2)+b_4^*\pi_{12}]}{G_{12}-i\omega}\right]\ , \tag{A21}$$

$$X_9=\int_{p_1}\int_{p_2}\frac{8b_3\chi_0^2}{\pi_1\pi_{12}(K_1-i\omega)}\left[\frac{\gamma_0^2a_3p_1^2}{\pi_1}-\frac{\gamma_0b_3^2\pi_1}{K_{12}-i\omega}+\frac{b_3L_1}{K_1-i\omega}\left[\gamma_0+\frac{b_3\pi_1}{K_{12}-i\omega}\right]\right]\ , \tag{A22}$$

$$X_{10}=\int_{p_1}\int_{p_2}\frac{8b_3\chi_0^2A_{12}}{\pi_2\pi_{12}(K_1-i\omega)}\left[\frac{b_3\gamma_0}{\lambda_0\chi_0^{-1}p_1^2}+\frac{b_3\gamma_0}{G_{12}-i\omega}+\frac{L_1(b_3\pi_2+b_3^*\pi_{12})}{\pi_1(K_1-i\omega)(G_{12}-i\omega)}\right]\ , \tag{A23}$$

$$X_{11}=\int_{p_1}\int_{p_2}\frac{8b_3\chi_0^2}{\pi_{12}(K_1-i\omega)}\left[\frac{\gamma_0b_3a_3p_2^2}{\pi_2(K_{12}-i\omega)}+\frac{\gamma_0b_3A_{12}}{\pi_1(G_{12}-i\omega)}+\frac{b_3L_2(L_{12}-a_3p_2^2)}{\pi_2(K_2-i\omega)(K_{12}-i\omega)}+\frac{A_{12}L_2(b_3\pi_1+b_3^*\pi_{12})}{\pi_1\pi_2(K_2-i\omega)(G_{12}-i\omega)}\right]\ . \tag{A24}$$

According to (A2) of Ref. 19 we consider h_0 in (A1) and (A15) as a function of τ_0. Up to two-loop order we find [compare (A6) of Ref. 19]

$$h_0(\tau_0)=\gamma_0[2J_1(\tau_0)+8(\gamma_0^2-4\tilde{u}_0)J_1(\tau_0)J_2(\tau_0)] \tag{A25}$$

which is to be substituted into the zeroth-order term of (A1). In the propagator of (A15) it suffices, within a two-loop calculation, to substitute only $h_0=2\gamma_0J_1(\tau_0)$. In the two-loop expressions (A16)–(A24) we have set $h_0=0$.

Equations (A25) and (2.7) can be used to calculate τ_0 in terms of r_0 up to two-loop order which can be substituted into the zeroth-order term of (A1). In the one-loop terms (A14) and (A15) it suffices to substitute (A7) of Ref. 19, and in the two-loop expressions we may replace τ_0 simply by r_0. Finally $\mathring{\Gamma}_{\psi\tilde{\psi}^*}$ is to be rewritten in terms of r_0-r_{0c} with r_{0c} being defined in the usual way.[8] For the purpose of determining only the pole terms of $\mathring{\Gamma}_{\psi\tilde{\psi}^*}$ in $d=4$ (see Appendix C), however, we may set $r_{0c}=0$ at the outset and work with τ_0 instead of r_0 provided that τ_0 is renormalized appropriately, see (C4).

APPENDIX B: DYNAMIC TWO-LOOP INTEGRALS

We shall consider all integrals at infinite cutoff and use dimensional regularization. For the purpose of calculating ζ_Γ we need the derivatives of the integrals (A14)–(A24) with respect to ω and τ_0, see (C10) and (C14). Within the minimal subtraction scheme it suffices to determine their simple poles $\sim\epsilon^{-1}$. The one-loop integrals are standard. Some of the dynamic two-loop integrals are more complicated than the model-E type[7] two-loop integrals. In the following we present the pole terms of some generic integrals. We shall keep the factor A_d, (2.16), unexpanded (with respect to ϵ) since it will be absorbed when turning to the renormalized couplings. We shall use the abbreviation

$$p_3^2\equiv(\mathbf{p}_1+\mathbf{p}_2)^2\ . \tag{B1}$$

By means of Feynman parametrization we have obtained

$$\int_{p_1}\int_{p_2}[(p_1^2+\tau_1)(p_2^2+\tau_2)(p_3^2+\tau_3)(\mu p_1^2+\nu p_2^2+\lambda p_3^2+\tau_4)]^{-1}$$
$$=A_d^2(4\epsilon)^{-1}\{\mu^{-1}\ln[\eta(\mu+\nu)(\mu+\lambda)]+\nu^{-1}\ln[\eta(\nu+\lambda)(\nu+\mu)]+\lambda^{-1}\ln[\eta(\lambda+\mu)(\lambda+\nu)]+O(\epsilon)\} \tag{B2}$$

with $\eta=(\mu\nu+\nu\lambda+\lambda\mu)^{-1}$,

$$\int_{p_1}\int_{p_2}[(p_1^2+\tau_1)(p_2^2+\tau_2)(p_3^2+\tau_3)]^{-1}=-A_d^2(4\epsilon)^{-1}(\tau_1^{1-\epsilon}+\tau_2^{1-\epsilon}+\tau_3^{1-\epsilon})[2\epsilon^{-1}+1+O(\epsilon)] , \tag{B3}$$

$$\int_{p_1}\int_{p_2}[(p_1^2+\tau_1)(p_2^2+\tau_2)(\mu p_1^2+\nu p_2^2+p_3^2+\tau_3)^2]^{-1}=A_d^2(4\epsilon)^{-1}\left[\ln\left[\frac{1+\nu+\mu+\nu\mu}{\nu+\mu+\nu\mu}\right]+O(\epsilon)\right] , \tag{B4}$$

$$\int_{p_1}\int_{p_2}[(p_1^2+\tau_1)^2(p_2^2+\tau_2)(\mu p_1^2+\nu p_2^2+p_3^2+\tau_3)]^{-1}=\frac{A_d^2\tau_1^{-\epsilon}}{4\epsilon(1+\nu)}\left[2\epsilon^{-1}-1+\xi\ln\left[\frac{\xi}{1+\xi}\right]+\ln\left[\frac{1+\nu}{1+\mu}\right]+O(\epsilon)\right] \tag{B5}$$

with $\xi=\nu+\mu+\nu\mu$. Many more integrals are needed in the complete two-loop calculation. Some of these integrals can be obtained from (B1)–(B5) by differentiation and/or by algebraic transformations of the integrands.

APPENDIX C: Z FACTORS IN TWO-LOOP ORDER

The main task is to determine the poles $\sim\epsilon^{-1}$ of Z_Γ up to two-loop order, i.e., up to $O(F^4,\gamma F^3,\gamma^2F^2,\gamma F^3,\gamma^4,\gamma^2 u,\gamma F u,F^2 u,u^2)$. This requires, in addition, the knowledge of the poles $\sim\epsilon^{-1}$ of the Z factors $\tilde Z_\psi$ or $\tilde Z_\psi^*=(\tilde Z_\psi)^*$ which renormalize the response fields[11,43,57,58]

$$\tilde\psi=\tilde Z_\psi^{-1/2}\tilde\psi_0,\quad \tilde\psi^*=(\tilde Z_\psi^*)^{-1/2}\tilde\psi_0^* . \tag{C1}$$

The renormalized counterpart of $\mathring{\Gamma}_{\psi\tilde\psi^*}(\omega)$ is

$$\Gamma_{\psi\tilde\psi^*}(\omega)=(Z_\psi\tilde Z_\psi^*)^{1/2}\mathring{\Gamma}_{\psi\tilde\psi^*}(\omega) , \tag{C2}$$

where the unrenormalized parameters $\tilde u_0,\gamma_0,\tau_0,\lambda_0,\Gamma_0,g_0$ in $\mathring{\Gamma}_{\psi\tilde\psi^*}$ are expressed in terms of renormalized ones according to (2.12)–(2.14) and[19]

$$\tilde u=\mu^{-\epsilon}\tilde Z_u^{-1}Z_\psi^2A_d\tilde u_0,\quad \tilde Z_u\tilde u=Z_u u+\tfrac{1}{2}Z_m Z_r^2 Z_\psi^2\gamma^2 , \tag{C3}$$

$$\tau=Z_\tau^{-1}\tau_0,\quad Z_\tau=Z_m Z_r . \tag{C4}$$

From statics[19,62] we know, for a two-component order parameter,

$$Z_\psi=1-16u^2/\epsilon , \tag{C5}$$

$$Z_m^{-1}=1-4\gamma^2/\epsilon-64\gamma^2 u/\epsilon^2 , \tag{C6}$$

$$Z_r=1+16u/\epsilon+16(28-5\epsilon)u^2/\epsilon^2 , \tag{C7}$$

$$Z_u=1+40u/\epsilon+64(25-8\epsilon)u^2/\epsilon^2 , \tag{C8}$$

$$Z_\tau^{-1}=Z_m^{-1}Z_r^{-1}=1-4(\gamma^2+4u)/\epsilon-16(12-5\epsilon)u^2/\epsilon^2 . \tag{C9}$$

The requirement that $\partial\Gamma_{\psi\tilde\psi^*}(\omega)/\partial\omega$ has no poles implies, according to (A1) and (C2),

$$(Z_\psi\tilde Z_\psi^*)^{1/2}-1=\text{poles of } 2(Z_\psi\tilde Z_\psi^*)^{1/2}\sum_{\nu=1}^{11}\frac{\partial X_\nu(\omega)}{\partial(-i\omega)} , \tag{C10}$$

where $X_\nu(\omega)$ is expressed in terms of renormalized parameters. The $\nu=2$ term yields the one-loop result

$$\tilde Z_\psi^*=1-\frac{8\gamma D}{(1+w)\epsilon} \tag{C11}$$

with D given by (3.15). Here we have corrected a misprint in Eq. (B3) of Ref. 11. From a calculation of the ω dependent two-loop terms ($\nu=5,\dots,11$) we have found

$$\begin{aligned}\tilde Z_\psi^*=1&-\frac{8\gamma D}{(1+w)\epsilon}+\frac{16u^2}{\epsilon}-\frac{Q_1}{\epsilon}\\&+\frac{8\gamma D^3(1+2w)}{\epsilon w(1+w)^3}\ln\left[\frac{1+2w}{(1+w)^2}\right]\\&-\frac{4\alpha_1}{\epsilon}\ln\left[\frac{w+2w^*}{2(w+w^*)}\right]\\&-\frac{4}{\epsilon}(\alpha_2+\gamma w DF^2\delta)\ln\left[\frac{w(w+2w^*)}{(w+w^*)^2}\right]\end{aligned} \tag{C12}$$

apart from pole terms $\sim\epsilon^{-2}$. The quantities δ, α_1, α_2, and Q_1 are given by (3.16), (3.18), (3.20), and (3.22).

Z_Γ can now be determined from the requirement that

$$\frac{\partial}{\partial\tau}\Gamma_{\psi\tilde\psi^*}(0)=(Z_\psi\tilde Z_\psi^*)^{1/2}Z_\tau\frac{\partial}{\partial\tau_0}\mathring{\Gamma}_{\psi\tilde\psi^*}(0) \tag{C13}$$

has no pole terms. According to (A1) this implies

$$\begin{aligned}Z_\Gamma^{-1}(Z_\psi\tilde Z_\psi^*)^{1/2}Z_\tau-1&=\text{poles of } 2\Gamma^{-1}(Z_\psi\tilde Z_\psi^*)^{1/2}Z_\tau\left[-\frac{1}{2}ig_0\frac{\partial h_0}{\partial\tau_0}\right.\\&\left.+\sum_{\nu=1}^{11}\frac{\partial X_\nu(0)}{\partial\tau_0}\right] ,\end{aligned} \tag{C14}$$

where the RHS is to be expressed in terms of renormalized parameters after the differentiation with respect to τ_0 has been performed. The $\nu=1$ and $\nu=2$ terms and the one-loop part of $h_0(\tau_0)$ yield the one-loop result

$$Z_\Gamma=1-\frac{4D^2}{w(1+w)\epsilon} . \tag{C15}$$

From a calculation of the two-loop terms we have found

$$Z_\Gamma = (\tilde{Z}_\psi^*)^{1/2} + \frac{2iFD}{\epsilon w(1+w)} - \frac{88u^2}{\epsilon} - \frac{Q_2}{2\epsilon} - \frac{2iFD^3(1+2w)}{\epsilon w^2(1+w)^3}\ln\left[\frac{1+2w}{(1+w)^2}\right] - \frac{2\eta_1}{\epsilon}\ln\left[\frac{w+2w^*}{2(w+w^*)}\right]$$
$$-\frac{2}{\epsilon}(\eta_2 - \tfrac{1}{2}iF^3D\delta)\ln\left[\frac{w(w+2w^*)}{(w+w^*)^2}\right] \tag{C16}$$

apart from the pole terms $\sim\epsilon^{-2}$. The quantities δ, η_1, η_2, and Q_2 are given by (3.16), (3.19), (3.21), and (3.23). Equations (C16) and (C12) lead to the expression for ζ_Γ, (3.14)–(3.23).

APPENDIX D: EFFECTIVE PARAMETERS

In this appendix more detailed information is given regarding the effective static and dynamic parameters which were computed by Sutter[63] (statics) and by Moser[64] (dynamics) according to the procedure described in Sec. IV.

1. Static parameters for the range $t \le 10^{-3}$

We shall abbreviate the RHS and LHS of (4.9) by $-\alpha^{\mathrm{theor}}(t)$ and $-\alpha^{\mathrm{expt}}(t)$, respectively. The flow equations (4.7) and (4.8) were integrated numerically and a least-squares fit was carried out by adjusting the initial values $u[t_0]$ and $\gamma[t_0]$ at $t_0=10^{-3}$ so as to minimize the squared deviations

$$\sigma^2 = \frac{1}{N}\sum_{i=1}^{N}[\alpha^{\mathrm{expt}}(t_i) - \alpha^{\mathrm{theor}}(t_i)]^2 , \tag{D1}$$

where N is the number of points t_i taken in the range of the fit. We have chosen this range as $10^{-4} < t < 10^{-3.5}$ and $N=450$. The results are quite insensitive to the precise value of N and to the choice of the range of the fit provided that $t<10^{-3}$. After the determination of $u[10^{-3}]$ and $\gamma[10^{-3}]$ the values $u[t]$ and $\gamma[t]$ were obtained for $10^{-9} \le t < 10^{-3}$ by numerical integration of the flow equations. This procedure was carried out at several pressures. The initial values $u[10^{-3}]$ and $\gamma[10^{-3}]$ are listed in Table I, and $u[t]$ and $\gamma[t]$ are shown in Fig. 3 for *SVP* (0.05 bars) and 28 bars, compare also the original Fig. 1 of Ref. 65 and Fig. 2 of Ref. 53. For numerical values and for intermediate pressures see Ref. 56.

2. Static parameters for the range $t > 10^{-3}$

In the range $t>10^{-3}$ the procedure suggested in Ref. 19 should be employed which yields "experimentally determined" values $(\gamma[t])^{\mathrm{expt}}$, i.e., $(\gamma[t])^2$ should be determined from (4.24) of Ref. 19,

$$\{(\gamma[t])^{\mathrm{expt}}\}^2 = \frac{(2-\zeta_r)\alpha^{\mathrm{expt}}(t)}{4-[2\zeta_r - 1 + (2-\zeta_r)\alpha^{\mathrm{expt}}(t)]F_+ - \beta_u \partial F_+/\partial u} , \tag{D2}$$

where the functions ζ_r, β_u, and F_+ on the RHS have the argument $u[t]$ [compare (6.8) of Ref. 19]. In (D2) the substitutions (4.12) and (4.13) should be made. For $t<10^{-3}$ the resulting $(\gamma[t])^{\mathrm{expt}}$ agrees essentially with $\gamma[t]$ obtained by integrating the RG flow equations (4.7) and (4.8). More precisely, $|\gamma[t]-(\gamma[t])^{\mathrm{expt}}|/\gamma[t]$ is less than 0.1% for $t<10^{-3}$, compare Tables I and II of Ref. 56. For $t>10^{-3}$, Eq. (D2) yields an effective $(\gamma[t])^{\mathrm{expt}}$ that provides an effective parametrization of the specific heat even beyond the range of applicability of the RG flow equation (4.8). For $t>10^{-2}$ this "experimentally determined" $(\gamma[t])^{\mathrm{expt}}$ differs significantly from the solution $\gamma[t]$ of the flow equations as is illustrated in Fig. 2 of Ref. 53 and in our Fig. 3. These departures are presumably due to finite-cutoff effects which are neglected in the RG flow equations of the minimally renormalized theory.

We have used (D2) in the following way. First we computed $u[t]$ by numerically integrating the RG flow equation (4.7) toward $t>10^{-3}$ with the initial values $u[10^{-3}]$ given in Table I. For $\alpha^{\mathrm{expt}}(t)$ we employed the experimental values according to (4.11). Then it is straightforward to calculate $\{(\gamma[t])^{\mathrm{expt}}\}^2$ from (D2). In Fig. 3 the resulting values for $u[t]$ and $(\gamma[t])^{\mathrm{expt}}$ are shown in the range $10^{-9}<t\le 10^{-1}$ for *SVP* (0.05 bars) and 28 bars. For comparison the solution $\gamma[t]$ of the RG flow equation (4.8) is also shown in Fig. 3 for $t \ge 10^{-3}$ (dashed lines). For numerical values see Table II and Ref. 56

3. Dynamic parameters

With the static parameters $u[t]$ and $\gamma[t]$ or $(\gamma[t])^{\mathrm{expt}}$ determined above it is now possible to determine the dynamic parameters $w[t]$ and $F[t]$ by means of a fit of $R_\lambda^{\mathrm{theor}}(t)$, (4.25), to $R_\lambda^{\mathrm{expt}}$, (4.26), as described in Sec. IV. The fitting procedure is that used in Ref. 24. First we have confined ourselves to the range $t \le t_0 = 10^{-3}$. Full-range fits were performed using the cell-*F* data for $t \le t_0 = 10^{-3}$ with the weights used by Tam and Ahlers.[24] The resulting parameters are plotted for *SVP* and 28 bar in Fig. 4. The qualitative features of $w'(l)$ and $f(l)$ agree with those found originally in Fig. 7 of Ref. 47, Fig. 1 of Ref. 58, and Fig. 2 of Ref. 66.

We have extended this procedure to the range $t \le t_0 = 10^{-2}$ by performing full-range fits to the cell-F data for $t \le t_0 = 10^{-2}$. Here we used $(\gamma[t])^{\text{expt}}$ instead of $\gamma[t]$. For $t \le 10^{-3}$ the resulting effective dynamic parameters w' and f agree closely with those determined from the fits with $t_0 = 10^{-3}$. In Fig. 5 the dynamic parameters are plotted for several pressures, and a few representative numerical values are listed in Table II. For additional values, also at intermediate pressures, see Ref. 56.

We consider these values, together with $u[t]$ and $(\gamma[t])^{\text{expt}}$, as the "standard parameters" of model F in the range $t \le 10^{-2}$. The differences with the parameters of Tam and Ahlers[24,29] are due to our more accurate static parameters. The conclusions by Tam and Ahlers about the agreement between the RG theory predictions and experiment are not affected by these differences.

4. Application to $T < T_\lambda$

Finally we briefly indicate how to employ the effective parameters shown in Figs. 3–5 to critical bulk phenomena below T_λ (at $k = \omega = 0$). Instead of (4.1) the flow parameter $l_- = l_-(t)$ below T_λ, $t < 0$, is most conveniently chosen as[19]

$$\frac{r(l_-)}{\mu^2 l_-^2} = -\frac{1}{2}, \quad \mu = \xi_0^{-1} . \tag{D3}$$

This leads to effective parameters $u(l_-)$, $\gamma(l_-)$, $w(l_-)$, and $F(l_-)$ in the expressions of renormalized correlation functions below T_λ (for example, in the amplitude of second-sound damping). From (4.1)–(4.3) and (D3) we obtain the relation, at given $t < 0$,

$$l_-(t) = l(-2t) , \tag{D4}$$

where l is the flow parameter above T_λ as defined by (4.1)–(4.4). Hence, at $t < 0$, we can identify the effective parameters $u(l_-)$, $\gamma(l_-)$, $w(l_-)$, and $F(l_-)$ explicitly in terms of the functions (4.6) and (4.16) taken at $-2t > 0$,

$$\begin{aligned} &u(l_-(t)) = u[-2t], \quad \gamma(l_-(t)) = \gamma[-2t] , \\ &w(l_-(t)) = w[-2t], \quad F(l_-(t)) = F[-2t] . \end{aligned} \tag{D5}$$

Thus Figs. 3–5 can be directly employed below T_λ after a simple shift of the temperature scale, compare also Fig. 1 of Ref. 65 and Fig. 1 of Ref. 67.

[1]P. C. Hohenberg and B. I. Halperin, Rev. Mod. Phys. **49**, 435 (1977).

[2]V. Dohm and R. Folk, Physica B **109&110**, 1549 (1982); P. C. Hohenberg, *ibid.* **109&110B**, 1436 (1982); V. Dohm and R. Folk, in *Advances in Solid State Physics,* edited by P. Grosse (Vieweg, Braunschweig, 1982), Vol. 22, p. 1.

[3]V. Dohm, J. Low Temp. Phys. **69**, 51 (1987).

[4]G. Ahlers and R. V. Duncan, in *Frontiers of Physics, Proceedings of the Landau Memorial Conference,* Tel Aviv, 1988, edited by E. Gotsman, Y. Ne'eman, and A. Voronel (Pergamon, Oxford, 1990), p. 219.

[5]E. Brézin, J. C. Le Guillou, and J. Zinn-Justin, in *Phase Transitions and Critical Phenomena,* edited by C. Domb and M. S. Green (Academic, New York, 1976), Vol. VI.

[6]D. J. Amit, *Field Theory, the Renormalization Group and Critical Phenomena* (World Scientific, Singapore, 1984).

[7]C. De Dominicis and L. Peliti, Phys. Rev. B **18**, 353 (1978).

[8]R. Schloms and V. Dohm, Nucl. Phys. **B328**, 639 (1989).

[9]R. Schloms and V. Dohm, Phys. Rev. B **42**, 6142 (1990).

[10]B. I. Halperin, P. C. Hohenberg, and E. D. Siggia, Phys. Rev. B **13**, 1299 (1976).

[11]V. Dohm, Z. Phys. B **61**, 193 (1985).

[12]D. Frank and V. Dohm, Phys. Rev. Lett. **62**, 1864 (1989).

[13]D. Frank and V. Dohm, Physica B **165&166**, 543 (1990).

[14]J. Pankert and V. Dohm, Europhys. Lett. **2**, 775 (1986); Phys. Rev. B **40**, 10 842 (1989); **40**, 10 856 (1989).

[15]R. Schloms, J. Pankert, and V. Dohm, Physica B **165&166**, 563 (1990).

[16]V. Dohm, and R. Folk, Phys. Rev. B **28**, 1332 (1983).

[17]G. Moser and R. Folk, Physica B **165&166**, 559 (1990); Phys. Rev. B **43**, 819 (1991).

[18]A. Onuki, J. Low Temp. Phys. **51**, 601 (1983).

[19]V. Dohm, Z. Phys. B **60**, 61 (1985).

[20]V. Dohm, Phys. Rev. B **29**, 1497 (1984).

[21]V. Dohm, in *Multicritical Phenomena,* edited by R. Pynn and A. Skjeltorp (Plenum, New York, 1984), p. 81.

[22]V. Dohm (unpublished).

[23]V. Dohm and R. Folk, Z. Phys. B **45**, 129 (1981).

[24]W. Y. Tam and G. Ahlers, Phys. Rev. B **33**, 183 (1986).

[25]J. Pankert and V. Dohm, Jpn. J. Appl. Phys. Suppl. **26-3**, 51 (1987).

[26]R. V. Duncan, G. Ahlers, and V. Steinberg, Phys. Rev. Lett. **58**, 377 (1987).

[27]J. A. Lipa and T. C. P. Chui, Phys. Rev. Lett. **58**, 1340 (1987).

[28]T. C. P. Chui, Q. Li, and J. A. Lipa, Jpn. J. Appl. Phys. Suppl. **26-3**, 371 (1987); J. A. Lipa, Q. Li, T. C. P. Chui, D. Marek, Nucl. Phys. **B** (Proc. Suppl.) **5A**, 31 (1988).

[29]W. Y. Tam and G. Ahlers, Phys. Rev. B **37**, 7898 (1988).

[30]D. Frank, M. Grabinski, V. Dohm, and M. Liu, Phys. Rev. Lett. **60**, 2336 (1988).

[31]G. Ahlers and R. V. Duncan, Phys. Rev. Lett. **61**, 846 (1988).

[32]D. Frank and V. Dohm, Z. Phys. (to be published).

[33]R. V. Duncan and G. Ahlers, Phys. Rev. B **43**, 7707 (1991).

[34]W. Y. Tam, Ph.D. thesis, University of California, Santa Barbara, 1985 (unpublished).

[35]J. Pankert, Ph.D. thesis, Technische Hochschule Aachen, 1986 (unpublished).

[36]J. Eggers, Diplom thesis, Technische Hochschule Aachen, 1987 (unpublished).

[37]R. V. Duncan, Ph.D. thesis, University of California, Santa Barbara, 1988 (unpublished).

[38]R. Schloms, Ph.D. thesis, Technische Hochschule Aachen, 1989 (unpublished).

[39]D. Frank, Ph.D. thesis, Technische Hochschule Aachen, 1989 (unpublished).

[40]Q. Li, T. C. P. Chui, and J. A. Lipa, Physica B **165&166**, 533 (1990).

[41]J. F. Nicoll and P. C. Albright, Phys. Rev. B **31**, 4576 (1985).

[42]J. C. Guillou and J. Zinn-Justin, J. Phys. (Paris) Lett. **46**, L137 (1985).

[43]R. Bausch, H. K. Janssen, and H. Wagner, Z. Phys. B **24**, 113 (1976).

[44]V. Dohm and R. A. Ferrell, Phys. Lett. **67A**, 387 (1978).
[45]V. Dohm, Z. Phys. B **31**, 327 (1978).
[46]V. Dohm, Z. Phys. B **33**, 79 (1979).
[47]V. Dohm and R. Folk, Z. Phys. B **40**, 79 (1980).
[48]A. A. Vladimirov, D. I. Kazakov, and O. V. Tarasov, Zh. Eksp. Teor. Fiz. **77**, 1035 (1979) [Sov. Phys. JETP **50**, 521 (1979)].
[49]H. J. Krause, R. Schloms, and V. Dohm, Z. Phys. B **79**, 287 (1990); **80**, 313 (1990).
[50]W. Y. Tam and G. Ahlers, Phys. Rev. B **32**, 5932 (1985).
[51]J. A. Lipa and T. C. P. Chui, Phys. Rev. Lett. **51**, 2291 (1983).
[52]R. Schloms and V. Dohm, Europhys. Lett. **3**, 413 (1987).
[53]V. Dohm and R. Schloms (unpublished).
[54]C. Bagnuls and C. Bervillier, Phys. Lett. **112A**, 9 (1985).
[55]A. J. Liu and M. E. Fisher, J. Stat. Phys. **58**, 431 (1990).
[56]V. Dohm and G. Moser, AIP document No. PAPS PRBMDO-44-2697-13, for 13 pages of extended versions of Tables I and II. Order by PAPS number and journal reference from American Institute of Physics, Physics Auxiliary Publication Service, 335 East 45th Street, New York, NY 10017. The price is $1.50 for a microfiche, or $5.00 for a photocopy. Airmail additional. Make checks payable to American Institute of Physics.
[57]R. A. Ferrell, N. Menyhárd, H. Schmidt, F. Schwabl, and P. Szépfalusy, Ann. Phys. (N.Y.) **47**, 565 (1968); B. I. Halperin and P. C. Hohenberg, Phys. Rev. **177**, 952 (1969).
[58]V. Dohm and R. Folk, Phys. Rev. Lett. **46**, 349 (1981).
[59]H. K. Janssen, Z. Phys. B **23**, 377 (1976).
[60]C. De Dominicis, J. Phys. (Paris) Colloq. **37**, C1-247 (1976).
[61]V. Dohm, Z. Phys. B **73**, 417 (1988).
[62]I. D. Lawrie, J. Phys. A **9**, 961 (1976).
[63]P. Sutter (private communication).
[64]G. Moser (private communication).
[65]V. Dohm, in *Proceedings of the Seventeenth International Conference on Low Temperature Physics,* edited by U. Eckern, A. Schmid, W. Weber, and H. Wühl (North-Holland, Amsterdam, 1984), p. 953.
[66]V. Dohm and R. Folk, Z. Phys. B **41**, 251 (1981).
[67]V. Dohm, Phys. Rev. Lett. **53**, 1379 (1984).